

Activation of CO₂ at Chromia-Nanocluster-Modified Rutile and Anatase

TiO₂

Michael Nolan^{1*} and Marco Fronzi^{1,2}

1: Tyndall National Institute, University College Cork, Lee Maltings, Prospect Row, Cork,
T12 R5CP, Ireland

2: International Research Centre for Renewable Energy, State Key Laboratory of Multiphase
Flow in Power Engineering, Xi'an Jiaotong University, Xi'an 710049, Shaanxi, China.

*michael.nolan@tyndall.ie

Abstract

Converting CO₂ to fuels is required to enable the production of sustainable fuels and to contribute to alleviating CO₂ emissions. In considering conversion of CO₂, the initial step of adsorption and activation by the catalyst is crucial. In addressing this difficult problem, we have examined how nanoclusters of reducible metal oxides supported on TiO₂ can promote CO₂ activation. In this paper we present density functional theory (DFT) simulations of CO₂ activation on heterostructures composed of clean or hydroxylated extended rutile and anatase TiO₂ surfaces modified with chromia nanoclusters. The heterostructures show non-bulk Cr and O sites in the nanoclusters and an upshifted valence band edge that is dominated by Cr 3d- O 2p interactions. We show that the supported chromia nanoclusters can adsorb and activate CO₂ and that activation of CO₂ is promoted whether the TiO₂ support is oxidised or

hydroxylated. Reduced heterostructures, formed by removal of oxygen from the chromia nanocluster, also promote CO₂ activation. In the strong CO₂ adsorption modes, the molecule bends giving O-C-O angles of 127 - 132° and elongation of C-O distances up to 1.30 Å; no carbonates are formed. The electronic properties show a strong CO₂-Cr-O interaction that drives the interaction of CO₂ with the nanocluster and induces the structural distortions. These results highlight that a metal oxide support modified with reducible metal oxide nanoclusters can activate CO₂, thus helping to overcome difficulties associated with the difficult first step in CO₂ conversion.

Keywords: DFT; CO₂ activation; adsorption; heterostructures

1. Introduction

CO₂ emissions from fossil fuels are the major cause of climate change and need to be eliminated in the near future to meet the targets of the COP21 Paris agreement to keep average global temperature increases below 2°C. Thus finding solutions to remove and store or use this CO₂ is a key concern. A solar driven photo- or thermochemical process for the conversion of CO₂ to CO, coupled with solar water splitting can produce synthesis gas, while direct conversion of CO₂ to liquid fuels would enable a sustainable approach to producing fuels and storing solar energy in high energy chemical bonds[1-11].

However, CO₂, as the most oxidised form of carbon, is highly stable and therefore activating it as part of the conversion process is difficult. In fact, to date, there are no widely available catalysts that can exploit solar energy (either directly or via thermochemical processes) to efficiently reduce CO₂ to useful chemicals. One successful example of a photocatalyst has been Pt-modified TiO₂ nanotubes[8, 12, 13] that produce methane. However, the efficiencies for

methane production are extremely low and Pt will never be an economically viable catalyst for large scale CO₂ conversion.

Copper has been shown to promote conversion of CO₂ into hydrocarbons, while many other metallic catalysts promote hydrogen evolution. More recently, catalysts based on oxide-derived Cu or Cu with mixed oxidation states have been shown to reduce CO₂ to useful molecules such as methane, methanol or ethanol [2, 14-26]. While this is encouraging, there is still an urgent need from a fundamental perspective to understand the factors that drive CO₂ activation and find materials to promote this process. Since a CO₂ anion (CO₂^{δ-}) is implicated in CO₂ conversion, using materials with excess electrons is one path to the development of CO₂ activation catalysts. These electrons could be produced through light excitation or formation of oxygen vacancies which release electrons to the catalyst. Transition metal-oxide based catalysts could show some promise in this regard; the work on Cu-based catalysts suggests a pathway towards exploiting reducible metal oxides for CO₂ conversion. It is also possible to promote CO₂ activation without necessarily producing an anionic species and this would be driven by interactions at suitable sites in the catalyst and/or suitable energy level alignments of the catalyst and CO₂.

Irrespective of the origin of the electrons that reduce CO₂, in any CO₂ conversion process the initial adsorption and activation of CO₂ is a key step. Thereafter there may be transfer of electron(s) to the CO₂ through light absorption or from excess electrons present in the catalyst after catalyst (pre-)reduction or in a combined PV+electrolysis system. Thus, the key challenge in fuel production from CO₂ is to discover catalysts that will promote the crucial first step, namely the adsorption and activation of CO₂.

Copper-based catalysts have been widely studied for CO₂ activation and conversion and this includes Cu metal, oxide-derived Cu and mixed oxidation state Cu [2, 14-26]. Modelling the

interaction of CO₂ with copper oxides uses density functional theory (DFT) to provide insights for further development of CO₂ activation catalysts. Wu *et al.* studied the adsorption of CO₂ at the Cu₂O (111) surface with oxygen vacancies [17], and found that dissociative adsorption was thermodynamically unfeasible. In addition, while a CO₂^{δ-} radical anion species can form on a defective surface, this is not stable. Wu *et al.* examined the adsorption of CO₂ at Cu₂O (111) using Hybrid DFT [21] and found adsorption only in non-activated form. This was confirmed by Bendavid and Carter [18]. Mishra *et al.* found similar results for CO₂ adsorption at Cu₂O (111), but reported strong chemisorption at the high energy Cu-O terminated (110) surface [14] and at the (011) surface of CuO [2]. Uzunova *et al.* studied the conversion of CO₂ to methanol on Cu₂O nanolayers and clusters [16] using Hybrid DFT. In the work of Favaro *et al.* [24] a model of Cu with subsurface oxygen was found to activate CO₂.

The adsorption of CO₂ molecules at different titania surfaces, including rutile and anatase, and nanostructures has also been well studied and the role of low coordinated sites, surface structure and oxygen vacancies has been discussed [27-32]. The presence of excess electrons and holes was shown to drive adsorption and activation of CO₂ at rutile (110) [33]. Yang *et al.* showed that sub-nm Pt clusters at the anatase (101) surface enhanced CO₂ activation through providing of additional adsorption sites and the transfer of electron density to the TiO₂ substrate [34]. Fewer studies exist for other metal oxide systems, but some examples include Cu/CeO₂ and Cu/CeO₂/TiO₂ [35], Cu/ZnO/Al₂O₃ [36] and dispersed CeO₂/TiO₂ [37]; the role of Ce³⁺ in visible light absorption, photogenerated charge separation and strengthening CO₂-surface bonding was highlighted.

Previously we have used first principles density functional theory (DFT) simulations to study heterostructured materials composed of TiO₂ (rutile or anatase) modified with metal oxide nanoclusters. In earlier work, the emphasis focussed on systems with predicted visible light absorption [38-49] and reduced charge recombination [39-43, 50, 51]. We have begun to extend

this work to study the interaction of molecules, such as CO₂, with these metal oxide nanocluster modified TiO₂ systems [38, 52]. We have investigated modified TiO₂ systems, *e.g.* ZrO₂-anatase, where CO₂ can adsorb and be activated [38] and reduced MnO_x-TiO₂ which show weak or unfavourable interactions with CO₂ [52]. There is therefore still much work to be done to understand the factors that drive CO₂ activation on metal oxides.

In the present paper, we use first principles density functional theory to examine in detail the interaction and activation of CO₂ at Cr₂O₃ nanocluster modified rutile and anatase TiO₂ surfaces, which are oxidised or hydroxylated. The interaction of CO₂ with reduced Cr₂O₃-TiO₂ heterostructures, upon loss of oxygen from the nanocluster, is also examined. While chromia is by far less studied for CO₂ adsorption compared to other oxides, there have a number of experimental surface science studies devoted to this topic [53-57]. These have discussed difficulties in obtaining high quality films of chromia or single crystals of Cr metal. Thus, chromia grown through oxidation of metallic Cr or chromia micropowders have been employed. These studies use infra red (IR) spectroscopy and thermal desorption spectroscopy (TDS) to examine the role of the termination of the chromia film on CO₂ adsorption. Termination with Cr enables strong adsorption of CO₂, as determined from TDS, with formation of carboxylate or carbonates. Termination with chromyl oxygen can bury these Cr sites and facilitates physisorption of linear CO₂, with a lower temperature TDS peak. The IR spectra show clear differences between the CO₂ adsorption modes. We find that chromia modified TiO₂ heterostructures are able to activate CO₂, causing O-C-O bending and elongation of C-O distances. This is independent of the state or identity of the TiO₂ surface, indicating that chromia nanoclusters drive CO₂ activation. In addition, reduced Cr₂O₃-TiO₂ heterostructures also activate CO₂. These findings thus show that transition metal oxide nanocluster modification of rutile and anatase TiO₂ produces heterostructures that can activate CO₂.

2. Methods

Following our approach from previous work on chromia-modified rutile and anatase[58] we prepare heterostructures of nanoclusters with Cr_4O_6 stoichiometry supported on rutile (110) and anatase (101); the Supporting Information contains full details. We use a three dimensional periodic surface slab within VASP [59-62], and a plane wave basis set. Projector augmented wave potentials[63, 64], with 4, 12, 6, 4 and 1 valence electrons for Ti, Cr, O, C and H are used [58]. The cut-off for the kinetic energy is 396 eV and the exchange-correlation functional is the Perdew-Wang 91[65] approximation. A Monkhorst-Pack ($2\times 1\times 1$) \mathbf{k} -point sampling grid is used. We apply the DFT+U approach [66] to describe the Ti 3d and Cr 3d states, with $U = 4.5$ eV for the Ti 3d states and 3.5 eV for the Cr 3d states [67, 68]. This DFT+U set-up is designed to recover a consistent description of the localisation of electrons in reduced cations rather than to recover the band gap. Convergence criteria for electronic and ionic relaxations are 0.0001 eV and 0.02 eV/Å. All calculations are spin polarised.

(2×4) and (4×2) surface supercell expansions are employed for rutile and anatase, respectively and the vacuum gap in all cases is 12 Å. The TiO_2 surfaces are unmodified oxidised or hydroxylated rutile (110) and anatase (101) surfaces [40, 58]. The free chromia nanoclusters are relaxed within the same computational described above, starting from different atomic arrangements. The most stable atomic structure of the free chromia Cr_4O_6 nanocluster is then adsorbed on the oxidised and hydroxylated TiO_2 surfaces in different adsorption configurations and these are relaxed. We then use the most stable relaxed chromia- TiO_2 heterostructures for subsequent study with CO_2 [39, 48, 51]. When clean rutile is modified with Cr_4O_6 , this is denoted **$\text{Cr}_4\text{O}_6\text{-o-rutile}$** and when hydroxylated rutile is modified with Cr_4O_6 , this is denoted **$\text{Cr}_4\text{O}_6\text{-oh-rutile}$** ; a similar nomenclature is used for anatase. The term **$\text{Cr}_2\text{O}_3\text{-TiO}_2$** indicates a

non-specific Cr₂O₃ nanocluster-modified TiO₂ heterostructure. Although the detailed study of the interaction of water at chromia-TiO₂ heterostructures is beyond the scope of this work, we have found that adsorption of water at Cr₄O₆-o-rutile and Cr₄O₆-oh-rutile is molecular with adsorption energies of -0.3 and -0.8 eV, so that there is a barrier to hydroxyl formation on adsorbed chromia.

The stability of the heterostructure is characterised by the nanocluster adsorption energy, E^{ads}

$$E^{\text{ads}} = E[(\text{Cr}_4\text{O}_6)\text{-TiO}_2] - \{E[(\text{Cr}_4\text{O}_6)] + E[\text{TiO}_2]\} \quad (1)$$

Where E[(Cr₄O₆)-TiO₂] is the computed total energy of Cr₄O₆ nanocluster-modified TiO₂, E(Cr₄O₆) is the computed total energy of the free Cr₄O₆ nanocluster and E(TiO₂) is the computed total energy of the unmodified TiO₂ (rutile/anatase) surface.

The CO₂ adsorption energy is defined in Eqn (2):

$$E^{\text{ads}} = E[\text{CO}_2@\text{Cr}_4\text{O}_6\text{-TiO}_2] - \{E[\text{Cr}_4\text{O}_6\text{-TiO}_2] + E[\text{CO}_2]\} \quad (2)$$

where E[CO₂@Cr₄O₆-TiO₂] is the computed total energy of CO₂ adsorbed at Cr₄O₆-modified TiO₂.

3. Results

We first briefly summarise the atomic structure of chromia-modified rutile and anatase TiO₂, in which the TiO₂ supports are oxidised or hydroxylated ½ ML coverage. These are shown in **Figures S1** and **S2** of the supporting information. Adsorption and relaxation of Cr₄O₆ on both TiO₂ surfaces gives adsorption energies of -4.25 eV and -5.85 eV on oxidised rutile and anatase and -1.08 eV and -2.21 eV on hydroxylated rutile and anatase, indicating strong nanocluster-surface interactions. The presence of surface hydroxyls and the migration of hydrogen to the support nanocluster reduce the energy gain upon chromia adsorption at hydroxylated surfaces.

Ti and Cr sites have the expected +4 and +3 oxidation states. Exceptions to this are Cr₄O₆-o-anatase, where a reduced Ti³⁺ and an oxidised Cr⁴⁺ cation are formed, and Cr₄O₆-oh-anatase, where 2 Cr²⁺ and 2 Cr⁴⁺ cations are present. In all heterostructures, the valence band edge is modified by the adsorption of Cr₄O₆ pushing the VB edge to higher energy. Oxygen vacancies can form readily in these systems, with formation energies of 0.22 eV and 1.95 eV on Cr₄O₆-o-rutile and Cr₄O₆-o-anatase, while these formation energies are 0.69 eV and 0.35 eV on Cr₄O₆-oh-rutile and Cr₄O₆-oh-anatase. Upon reduction, heterostructures of chromia on oxidised and hydroxylated supports show the presence of reduced Ti³⁺ and Cr²⁺ species.

3.1 Adsorption and Activation of CO₂ at Chromia-Modified Rutile (110) and Anatase (101)

3.1.1 CO₂ Adsorption at Cr₄O₆-modified rutile

Figure 1 shows the atomic structure for the two most stable CO₂ adsorption modes that we have found at Cr₄O₆-o-rutile (110) (Figure 1(a), (b)), modes I and II) and Cr₄O₆-oh-rutile (110) (Figure 1(c), (d) modes I and II). The computed adsorption energies for the two CO₂ adsorption modes on Cr₄O₆-o-rutile (110) are -0.63 eV and -0.91 eV for modes I and II. In Cr₄O₆-oh-rutile (110), the CO₂ adsorption energies are -0.92 eV and -0.31 eV for modes I and II. Clearly the modification of rutile with chromia produces heterostructures that show moderately strong adsorption capability for CO₂, which is the first requirement for CO₂ conversion. These energies are 0 K DFT energy differences and if we include the zero point energy corrections (ZPE) for CO₂ adsorption these are only on the order of 0.03 eV which makes no significant change to the adsorption energies at chromia-modified TiO₂. If we compare with the available

work on CO₂ adsorption at chromia, then the moderately strong adsorption energies can arise from the availability of Cr sites in the nanocluster to interact with oxygen of CO₂, in a similar to the stronger Cr-CO₂ interaction described experimentally in refs[54-56].

We have examined multiple CO₂ adsorption sites on each chromia-TiO₂ system and other, less favourable adsorption modes are shown in Figures S3 and S4 and the energies relative to the most stable adsorption mode are shown in Table S1 of the Supporting Information. Even though these adsorption modes are less stable than those shown in Figure 1, we can see that they still generally show moderate CO₂ adsorption energies and similar adsorption structures, so that CO₂ adsorption and activation at multiple sites of chromia-modified TiO₂ is likely. We have also relaxed the adsorption structures in Figure 1 with no +U correction and find that the adsorption of CO₂ and the changes to its geometry are not influenced by the inclusion of the +U correction into the computational set-up.

In discussing the adsorption structure of CO₂, we focus on the change in molecular C-O distances and the O-C-O angle. In gas phase CO₂, the C-O distances are 1.16 Å, while the O-C-O angle is 180°. On Cr₄O₆-o-rutile, CO₂ adsorption in mode I results in the C-O distances elongating to 1.27 and 1.23 Å, while the O-C-O angle is 132°. One oxygen atom of CO₂ binds to a Cr site in the nanocluster, with a Cr-O distance of 2.05 Å. Finally, the C-O distance to the nanocluster is 1.44 Å. In adsorption mode II, the C-O distances in adsorbed CO₂ both lengthen to 1.27 Å and the O-C-O angle is 130°. Both oxygen atoms of the molecule bind to Cr sites in the nanocluster, with Cr-O distances of 2.08 Å and 2.13 Å. The carbon of CO₂ shows a C-O distance to the nanocluster of 1.39 Å. Thus, the adsorption of CO₂ causes a lengthening of molecular C-O distances and bending of the molecule, characteristic of CO₂ activation [4, 69]. We also note that the deviation from linearity in the O-C-O angle increases with the strength of CO₂ adsorption.

Finally, we have computed the vibrational frequencies of adsorbed CO₂; for reference our computed vibrational modes for gas-phase CO₂ are 2354, 1325, and 632 cm⁻¹ and the experimental CO₂ vibrational modes are 2349, 1333 and 667 cm⁻¹ [70] so that our gas phase CO₂ vibrational modes are in good agreement with experiment. In mode I, the computed vibrational modes are 1720, 1221, 791 and 767 cm⁻¹, while in mode II, the vibrational modes are 1589, 1226, 921 and 803 cm⁻¹. We note the large red shift of up to 765 cm⁻¹ in the C=O stretching mode and the lifting of the degeneracy of the O-C-O bending mode upon adsorption of CO₂ on the chromia nanocluster. The C-O elongation is not as large in mode I so the shift in the C=O stretching mode is correspondingly smaller. These results strongly indicate that CO₂ adsorbs in an activated mode.

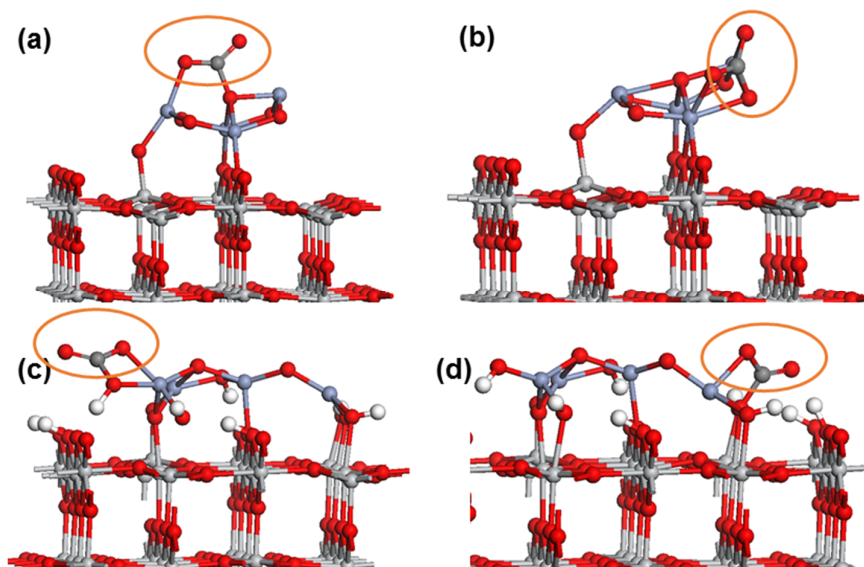


Figure 1: Relaxed atomic structures for CO₂ adsorbed in two adsorption modes at (a), (b) Cr₄O₆-o-rutile and (c), (d) Cr₄O₆-oh-rutile. The colour scheme is Ti: grey spheres, O: red spheres, Cr: blue spheres and C: grey spheres. The ring shows the CO₂ molecule.

If we turn to activation of CO₂ at the Cr₄O₆-oh-rutile (110) heterostructure, adsorption of CO₂ in mode I (Figure 1(c)) results in an elongation of the molecular C-O distances to 1.21 and 1.31 Å, while the O-C-O angle is bent, with an angle of 132°. The C-O distance to the nanocluster is 1.44 Å and the Cr-O distance to the molecule is 1.99 Å. In adsorption mode II (Figure 1(d)), the C-O distances are 1.24 and 1.30 Å, while the O-C-O angle is 128°. We note the stronger elongation of one C-O distance upon adsorption at Cr₄O₆-oh-rutile compared to adsorption at Cr₄O₆-o-rutile. The oxygen involved is bound to Cr in the nanocluster, so this extra interaction permits a lengthening of the C-O bond.

The computed vibrational modes are 1774, 1152, 899, 796 cm⁻¹ and 1658, 1206, 927 and 772 cm⁻¹ for modes I and II, respectively. These are similar to CO₂ adsorption at the Cr₄O₆-o-rutile heterostructure and the non-uniform elongation of the C-O distances results in a smaller red shift in the C=O stretching mode. Thus, the interaction of CO₂ at chromia-modified rutile results in strong adsorption and activation of the molecule and this is irrespective of the state of the support. The activation of CO₂ is accompanied by distortions to the molecule, namely C-O bond elongation and O-C-O bending.

3.1.2 CO₂ Adsorption at Cr₄O₆-modified anatase

Figure 2 shows the atomic structure for two CO₂ adsorption modes at Cr₄O₆-o-anatase (101) (Figure 2(a), (b)), modes I and II) and Cr₄O₆-oh-anatase (101) (Figure 2(c), (d) modes I and II). On Cr₄O₆-o-anatase (101), adsorption of CO₂ in mode I has a rather large adsorption energy of -2 eV, suggesting that the CO₂ may be over stabilised upon adsorption. In mode II, the computed adsorption energy is -0.13 eV. However, we note for adsorption mode II that a CO molecule is directly formed and this process is exothermic. The C-O distance in the free CO molecule is 1.14 Å.

In adsorption mode I, the C-O distances elongate to 1.26 and 1.28 Å and the O-C-O angle is 133°. The C-O distance to the nanocluster is 1.39 Å and the Cr-O distance to the molecule is 2.13 Å. Computed vibrational modes of adsorbed CO₂ in mode I are 1617, 1201, 915 and 906 cm⁻¹, which again show activation of adsorbed CO₂.

After CO₂ adsorption on Cr₄O₆-oh-anatase (101), the computed adsorption energies are -0.71 eV and -1.11 eV for modes I and II, respectively. In a similar fashion to the results on chromia-rutile, the availability of Cr sites in the nanocluster permits interaction with CO₂. In mode I the molecular C-O distances are 1.25 and 1.28 Å, with an O-C-O bending angle of 127°. In mode II, the C-O distances are 1.24 and 1.29 Å and the O-C-O bending angle is 128°. Computed vibrational modes for adsorbed CO₂ are 1628, 1246, 908 and 799 cm⁻¹ on Cr₄O₆-o-anatase and 1642, 1243, 959 and 777 cm⁻¹ on Cr₄O₆-oh-anatase. Thus, the activation of CO₂ at chromia modified anatase is not dependence on the state of the TiO₂ support.

We recall that Cr₄O₆-o-anatase has a reduced Ti³⁺ and a Cr⁴⁺ cation [58]. Upon formation of activated CO₂ (mode I), both cations are partially reoxidised and there is a charge redistribution, with a transfer of 0.5 electrons to CO₂. Upon formation of CO, examination of the computed indicates reoxidation of the Cr²⁺ and Ti³⁺, with a transfer of 2 electrons to adsorbed CO₂ which promotes the formation of CO.

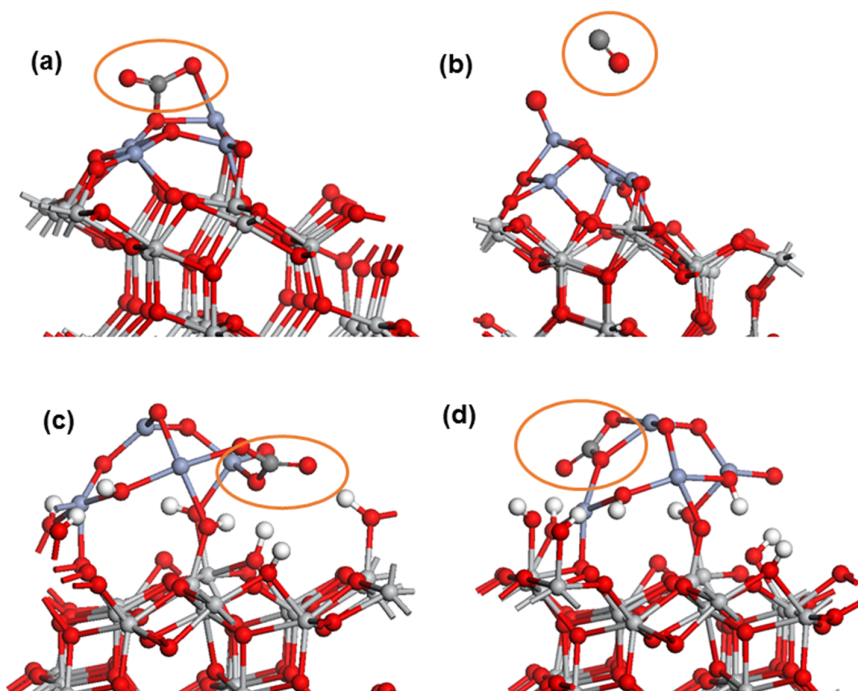


Figure 2: Relaxed atomic structures for CO₂ adsorbed in two adsorption modes at (a), (b) Cr₄O₆-o-anatase and (c), (d) Cr₄O₆-oh-anatase. The colour scheme is the same as Figure 1. The ring shows the CO₂ molecule.

3.2 Adsorption and Activation of CO₂ at Reduced Chromia-Modified Rutile and Anatase

We finally consider the adsorption of CO₂ at two examples of reduced Cr₂O₃-TiO₂, where the rutile and anatase supports are hydroxylated. Since in any process for conversion of CO₂, water is likely to be used as a proton source, the supports will most likely have some coverage of water present and this is accounted for by using our ½ ML hydroxylated supports. In addition, the reduction energies of chromia-modified hydroxylated TiO₂ are moderate, so this needs to be taken into account when investigating CO₂ activation.

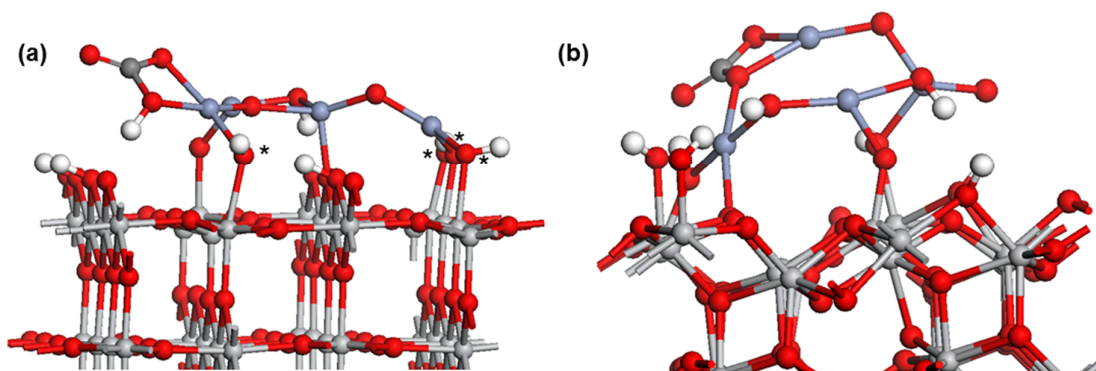


Figure 3: Relaxed atomic structures for CO₂ adsorbed at (a) reduced Cr₄O₅-oh-rutile and (b) reduced Cr₄O₅-oh-anatase. The colour scheme is the same as Figure 1.

Figure 3 shows the atomic structure of CO₂ adsorbed at reduced Cr₄O₅-oh-rutile (110) and Cr₄O₅-oh-anatase (101). The computed CO₂ adsorption energies are -0.6 eV and -1.85 eV on rutile and anatase, respectively. The presence of the oxygen vacancy in the chromia nanocluster promotes adsorption of CO₂, particularly on the anatase support. Hydrogen atoms from the hydroxyl sites do not migrate to the adsorbed CO₂.

The C-O distances in the molecule elongate to 1.21 and 1.29 Å upon adsorption at Cr₄O₅-oh-rutile and to 1.24 and 1.31 Å upon adsorption at Cr₄O₅-oh-anatase. The corresponding O-C-O angles are 133° (rutile) and 127° (anatase). The third C-O distance to the nanocluster is 1.47 and 1.37 Å in Cr₄O₅-oh-rutile and Cr₄O₅-oh-anatase.

When we examine the oxidation states of the Ti and Cr cations in the supports and the nanocluster, the adsorption of CO₂ does not result in any significant change in the oxidation states of Ti and Cr cations; such changes are on the order of < 0.1 electrons so that reduced cation species persist. Thus, we suggest that there is some charge redistribution upon bonding with CO₂.

4. Discussion and Conclusion

Finding materials that can activate CO₂ is of high interest for using CO₂ as a feedstock for sustainable fuel production. The present study shows that CO₂ can adsorb and activate at chromia nanocluster modified rutile and anatase TiO₂ heterostructures. We characterise the activation of CO₂ by the strength of adsorption, the elongation of C-O distances, the bending of the O-C-O angle and the red shift in the C=O stretching mode. In almost all cases we find moderately strong CO₂ adsorption; the exception is at Cr₄O₆-o-anatase. The C-O distances elongate, with a particularly strong elongation on chromia-anatase heterostructures, where the C-O distances elongate up to 1.30 Å. On chromia-rutile, the elongation is not uniform, with one C-O bond clearly longer than the other. The O-C-O angle always shows significant bending, where we find angles in the range of 127 – 132°. The state of the TiO₂ support, whether perfect or hydroxylated, and reduction of the chromia nanocluster, do not influence the adsorption and activation of CO₂ and it is therefore the chromia nanocluster modifier that promotes CO₂ adsorption.

The supported nanoclusters offer some advantageous properties for CO₂ activation. Firstly, there are low coordinated metal and oxygen sites in such non-bulk like structures, which have the potential to be active towards molecular adsorption. Secondly the presence of non-bulk like atomic environments can modify the electronic structure relative to bulk materials and the support. To examine any electronic structure effects, we show the projected electronic density of states (PEDOS) for the examples of CO₂ adsorption in mode I on C₄O₆-oh-rutile and in mode I on Cr₄O₆-oh-anatase in Figures 4 and 5. We recall that in the heterostructures, there are Cr₄O₆-derived electronic states above the valence band edge of the TiO₂ support. The PEDOS show

that these states persist upon adsorption of CO₂. Importantly, the CO₂ PEDOS, decomposed into C 2p and O 2p contributions, shows broad PEDOS peaks which are indicative of strong interactions between CO₂ and the oxide nanocluster. In particular, the O 2p states are found in the same energy range as the Cr₄O₆ states, while the C 2p PEDOS is also broad in the region from -2 eV to -6 eV below the highest occupied states. Thus, it is clear that the position of the Cr₄O₆-TiO₂ electronic states is suitable to allow hybridisation with the C 2p and O 2p states of CO₂. We note also that some supported chromia nanoclusters have Cr²⁺ oxidation states, and reducing the heterostructure through oxygen removal produces Ti³⁺ and Cr²⁺ sites. After adsorption of CO₂, we find that there can be reoxidation of these reduced cations, particularly in the case of CO formation, in which electron transfer from reduced Ti and Cr species is found. In other cases there is a redistribution of charge upon CO₂ adsorption. Thus, the chromia-modified TiO₂ heterostructures display suitable characteristics, namely active sites, suitable energy level positions and variable cation oxidation states which promote the adsorption and activation of CO₂.

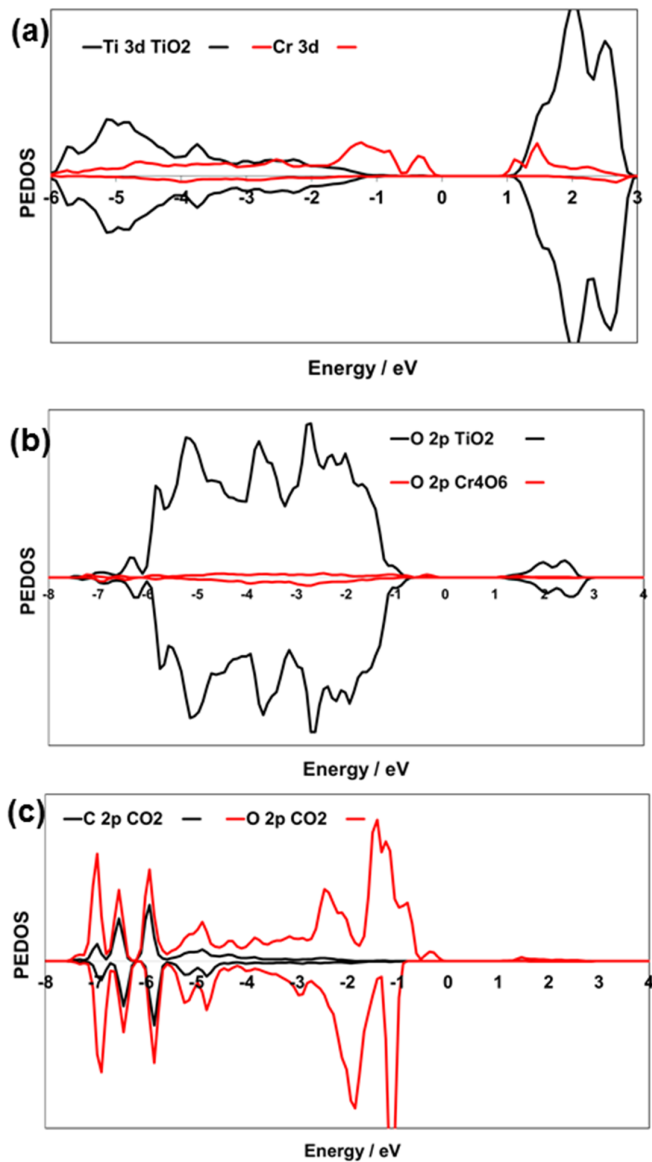


Figure 4: Projected electronic density of states for CO₂ adsorbed on Cr₄O₆-oh-rutile (110).

The PEDOS is shown for Cr 3d and O 2p states in chromia, Ti 3d and O 2p states in TiO₂ and C and O 2p states in adsorbed CO₂. The zero of energy is the top of the highest occupied states.

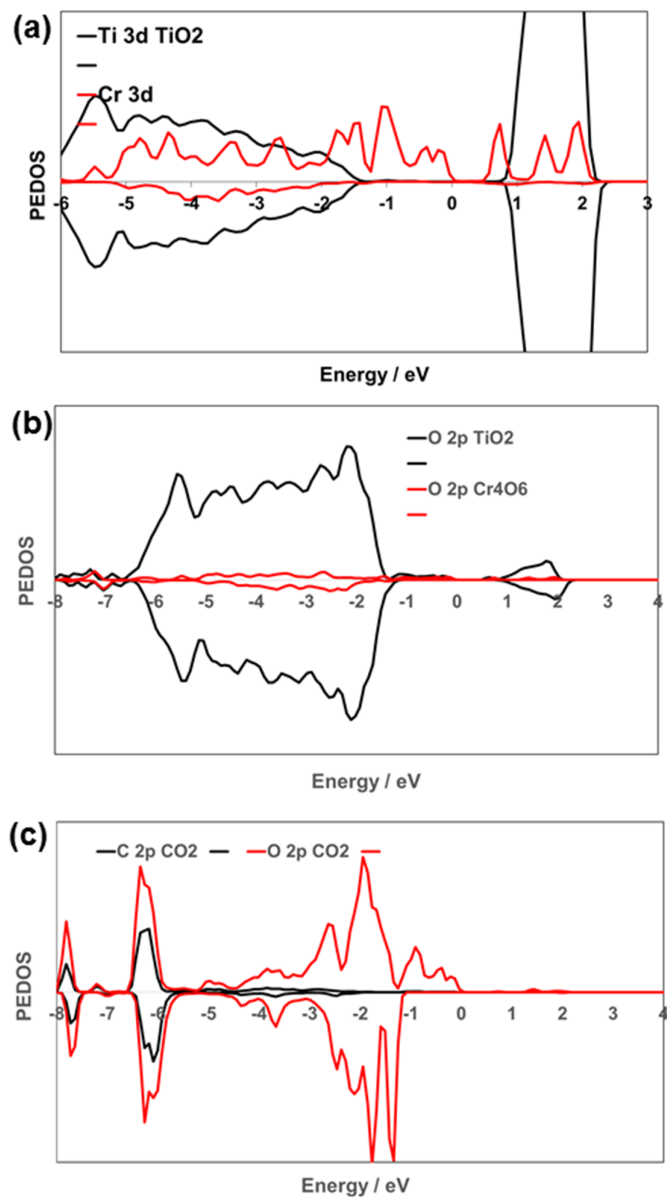


Figure 5: Projected electronic density of states for CO₂ adsorbed on Cr₄O₆-oh-anatase (110). The PEDOS is shown for Cr 3d and O 2p states in chromia, Ti 3d and O 2p states in TiO₂ and C and O 2p states in adsorbed CO₂. The zero of energy is the top of the highest occupied states.

In conclusion, the results of DFT studies of CO₂ adsorption at chromia-modified rutile and anatase TiO₂ surfaces show that these heterostructures are able to adsorb and activate CO₂, thus contributing to expanding the range of oxide-based structures that can promote the critical first step in the conversion of CO₂.

Acknowledgements

We acknowledge support from Science Foundation Ireland through the US-Ireland R&D Partnership Program Project SusChem SFI 14/US/E2915 and the M-ERA.net co-fund program, grant number SFI 16/M-ERA/2918, H2020 Grant Agreement 685451. Access to the computational resources at the Science Foundation Ireland/Higher Education Authority funded Irish Centre for High End Computing is acknowledged.

References

- [1] X. Chang, T. Wang, J. Gong, CO₂ photo-reduction: insights into CO₂ activation and reaction on surfaces of photocatalysts, *Energy Environ Sci.*, 9 (2016) 2177-2196.
- [2] A.K. Mishra, A. Roldán, N.H. de Leeuw, CuO Surfaces and CO₂ Activation: A Dispersion-Corrected DFT+U Study, *J. Phys. Chem. C*, 120 (2016) 2198-2214.
- [3] S. Kwon, P. Liao, P.C. Stair, R.Q. Snurr, Alkaline-earth metal-oxide overlayers on TiO₂: application toward CO₂ photoreduction, *Catal. Sci. Technol.*, 6 (2016) 7885-7895.
- [4] C. Kunkel, F. Viñes, F. Illas, Transition metal carbides as novel materials for CO₂ capture, storage, and activation, *Energy Environ Sci.*, 9 (2016) 141-144.
- [5] C. Peng, G. Reid, H. Wang, P. Hu, Perspective: Photocatalytic reduction of CO₂ to solar fuels over semiconductors, *J. Chem. Phys.*, 147 (2017) 030901.
- [6] H. Zhao, F. Pan, Y. Li, A review on the effects of TiO₂ surface point defects on CO₂ photoreduction with H₂O, *Journal of Materiomics*, 3 (2017) 17-32.
- [7] C. Song, Global Challenges and Strategies for Control, Conversion and Utilization of CO₂ for Sustainable Development Involving Energy, Catalysis, Adsorption and Chemical Processing, *Cat. Today* 115 (2006) 2-32.
- [8] S.C. Roy, O.K. Varghese, M. Paulose, C.A. Grimes, Toward solar fuels: photocatalytic conversion of carbon dioxide to hydrocarbons, *ACS Nano*, 4 (2010) 1259-1278.
- [9] M. Mikkelsen, M. Jorgensen, F.C. Krebs, The teraton challenge. A review of fixation and transformation of carbon dioxide, *Energy Environ Sci.*, 3 (2010) 43-81.
- [10] S.N. Habisreutinger, L. Schmidt-Mende, J.K. Stolarczyk, Photocatalytic Reduction of CO₂ on TiO₂ and Other Semiconductors, *Angew. Chem. Int. Ed.*, 52 (2013) 7372-7408.

- [11] A. Goepfert, M. Czaun, J.-P. Jones, G.K. Surya Prakash, G.A. Olah, Recycling of carbon dioxide to methanol and derived products - closing the loop, *Chem. Soc. Rev.*, 43 (2014) 7995-8048.
- [12] O.K. Varghese, M. Paulose, T.J. LaTempa, C.A. Grimes, High-Rate Solar Photocatalytic Conversion of CO₂ and Water Vapor to Hydrocarbon Fuels, *Nano Lett.*, 9 (2009) 731-737.
- [13] O.K. Varghese, M. Paulose, T.J. LaTempa, C.A. Grimes, High-Rate Solar Photocatalytic Conversion of CO₂ and Water Vapor to Hydrocarbon Fuels, *Nano Lett.*, 10 (2010) 750-750.
- [14] A.K. Mishra, A. Roldán, N.H.d. Leeuw, A density functional theory study of the adsorption behaviour of CO₂ on Cu₂O surfaces, *J. Chem. Phys.*, 145 (2016) 044709.
- [15] A.A. Peterson, F. Abild-Pedersen, F. Studt, J. Rossmeisl, J.K. Nørskov, How copper catalyzes the electroreduction of carbon dioxide into hydrocarbon fuels, *Energy Environ Sci.*, 3 (2010) 1311-1315.
- [16] E.L. Uzunova, N. Seriani, H. Mikosch, CO₂ conversion to methanol on Cu(I) oxide nanolayers and clusters: an electronic structure insight into the reaction mechanism, *Phys. Chem. Chem. Phys.*, 17 (2015) 11088-11094.
- [17] H. Wu, N. Zhang, H. Wang, S. Hong, Adsorption of CO₂ on Cu₂O (111) oxygen-vacancy surface: First-principles study, *Chem. Phys. Lett.*, 568 (2013) 84-89.
- [18] L.I. Bendavid, E.A. Carter, CO₂ Adsorption on Cu₂O(111): A DFT+U and DFT-D Study, *J. Phys. Chem. C*, 117 (2013) 26048-26059.
- [19] H. Wu, N. Zhang, H. Wang, S. Hong, Adsorption of CO₂ on Cu₂O (111) oxygen-vacancy surface: First-principles study, *Chem. Phys. Lett.*, 568-569 (2013) 84-89.
- [20] L. Liu, C. Zhao, Y. Li, Spontaneous Dissociation of CO₂ to CO on Defective Surface of Cu(I)/TiO_{2-x} Nanoparticles at Room Temperature, *J. Phys. Chem. C*, 116 (2012) 7904-7912.
- [21] H. Wu, N. Zhang, Z. Cao, H. Wang, S. Hong, The adsorption of CO₂, H₂CO₃, HCO₃⁻ and CO₃²⁻ on Cu₂O (111) surface: First-principles study, *Int. J. Quantum Chem*, 112 (2012) 2532-2540.
- [22] D. Gao, I. Zegkinoglou, N.J. Divins, F. Scholten, I. Sinev, P. Grosse, B. Roldan Cuenya, Plasma-Activated Copper Nanocube Catalysts for Efficient Carbon Dioxide Electroreduction to Hydrocarbons and Alcohols, *ACS Nano*, 11 (2017) 4825-4831.
- [23] H. Mistry, A.S. Varela, C.S. Bonifacio, I. Zegkinoglou, I. Sinev, Y.-W. Choi, K. Kisslinger, E.A. Stach, J.C. Yang, P. Strasser, B. Roldan Cuenya, Highly selective plasma-activated copper catalysts for carbon dioxide reduction to ethylene, *Nature Communications*, 7 (2016) 12123.
- [24] M. Favaro, H. Xiao, T. Cheng, W.A. Goddard, J. Yano, E.J. Crumlin, Subsurface oxide plays a critical role in CO₂ activation by Cu(111) surfaces to form chemisorbed CO₂, the first step in reduction of CO₂, *Proceedings of the National Academy of Sciences*, 114 (2017) 6706-6711.
- [25] L. Wang, K. Gupta, J.B.M. Goodall, J.A. Darr, K.B. Holt, In situ spectroscopic monitoring of CO₂ reduction at copper oxide electrode, *Faraday Discuss.*, 197 (2017) 517-532.
- [26] S.A. Akhade, W. Luo, X. Nie, A. Asthagiri, M.J. Janik, Theoretical insight on reactivity trends in CO₂ electroreduction across transition metals, *Catal. Sci. Technol.*, 6 (2016) 1042-1053.
- [27] V.P. Indrakanti, Photoinduced activation of CO₂ on TiO₂ surfaces: Quantum chemical modeling of CO₂ adsorption on oxygen vacancies, *Fuel Process. Technol.*, 92 (2011) 805-811
- [28] W. Pipornpong, R. Wanbayor, V. Ruangpornvisuti, Adsorption of CO₂ on the perfect and oxygen vacancy defect surfaces of anatase TiO₂ and its photocatalytic mechanism of conversion to CO, *Appl. Surf. Sci.*, 257 (2011) 10322-10328.
- [29] D. Lee, Y. Kanai, Role of Four-Fold Coordinated Titanium and Quantum Confinement in CO₂ Reduction at Titania Surface, *J. Am. Chem. Soc.*, 134 (2012) 20266-20269.
- [30] U. Tumuluri, J.D. Howe, W.P. Mounfield, M. Li, M. Chi, Z.D. Hood, K.S. Walton, D.S. Sholl, S. Dai, Z. Wu, Effect of Surface Structure of TiO₂ Nanoparticles on CO₂ Adsorption and SO₂ Resistance, *ACS Sustainable Chemistry & Engineering*, 5 (2017) 9295-9306.
- [31] X. Lin, Z.-T. Wang, I. Lyubinetsky, B.D. Kay, Z. Dohnalek, Interaction of CO₂ with oxygen adatoms on rutile TiO₂(110), *Phys. Chem. Chem. Phys.*, 15 (2013) 6190-6195.
- [32] X. Lin, Y. Yoon, N.G. Petrik, Z. Li, Z.-T. Wang, V.-A. Glezakou, B.D. Kay, I. Lyubinetsky, G.A. Kimmel, R. Rousseau, Z. Dohnalek, Structure and Dynamics of CO₂ on Rutile TiO₂(110)-1×1, *J. Phys. Chem. C*, 116 (2012) 26322-26334.

- [33] W.-J. Yin, B. Wen, S. Bandaru, M. Krack, M.W. Lau, L.-M. Liu, The Effect of Excess Electron and hole on CO₂ Adsorption and Activation on Rutile (110) surface, *Scientific Reports*, 6 (2016) 23298.
- [34] C.-T. Yang, B.C. Wood, V.R. Bhethanabotla, B. Joseph, CO₂ Adsorption on Anatase TiO₂ (101) Surfaces in the Presence of Subnanometer Ag/Pt Clusters: Implications for CO₂ Photoreduction, *J. Phys. Chem. C*, 118 (2014) 26236-26248.
- [35] J. Graciani, K. Mudiyansele, F. Xu, A.E. Baber, J. Evans, S.D. Senanayake, D.J. Stacchiola, P. Liu, J. Hrbek, J.F. Sanz, J.A. Rodriguez, Highly active copper-ceria and copper-ceria-titania catalysts for methanol synthesis from CO₂, *Science*, 345 (2014) 546-550.
- [36] M. Behrens, F. Studt, I. Kasatkin, S. Kühl, M. Hävecker, F. Abild-Pedersen, S. Zander, F. Girgsdies, P. Kurr, B.-L. Kniep, M. Tovar, R.W. Fischer, J.K. Nørskov, R. Schlögl, The Active Site of Methanol Synthesis over Cu/ZnO/Al₂O₃ Industrial Catalysts, *Science*, 336 (2012) 893-897.
- [37] Y. Wang, J. Zhao, T. Wang, Y. Li, X. Li, J. Yin, C. Wang, CO₂ photoreduction with H₂O vapor on highly dispersed CeO₂/TiO₂ catalysts: Surface species and their reactivity, *J. Catal.*, 337 (2016) 293-302.
- [38] M. Fronzi, W. Daly, M. Nolan, Reactivity of metal oxide nanocluster modified rutile and anatase TiO₂: Oxygen vacancy formation and CO₂ interaction, *Applied Catalysis A*, 521 (2016) 240-249.
- [39] M. Nolan, A. Iwaszuk, A.K. Lucid, J.J. Carey, M. Fronzi, Design of novel visible light active photocatalyst materials: surface modified TiO₂, *Adv. Mater.*, 28 (2016) 5425-5446.
- [40] M. Fronzi, A. Iwaszuk, A. Lucid, M. Nolan, Metal oxide nanocluster-modified TiO₂ as solar activated photocatalyst materials, *J. Phys.: Condens. Matter*, 28 (2016) 074006.
- [41] H. Tada, Q. Jin, A. Iwaszuk, M. Nolan, Molecular-scale transition metal oxide nanocluster surface-modified titanium dioxide as solar-activated environmental catalysts, *J. Phys. Chem. C*, 118 (2014) 12077-12086.
- [42] A. Iwaszuk, A.K. Lucid, K.M. Razeeb, M. Nolan, First principles investigation of anion-controlled red shift in light absorption in ZnX (X = O, S, Se) nanocluster modified rutile TiO₂, *J. Mater. Chem. A*, 2 (2014) 18796-18805.
- [43] A. Iwaszuk, M. Nolan, SnO-nanocluster modified anatase TiO₂ photocatalyst: exploiting the Sn(II) lone pair for a new photocatalyst material with visible light absorption and charge carrier separation, *J. Mater. Chem. A*, 1 (2013) 6670-6677.
- [44] A. Iwaszuk, M. Nolan, Q. Jin, M. Fujishima, H. Tada, Origin of the Visible-Light Response of Nickel(II) Oxide Cluster Surface Modified Titanium(IV) Dioxide, *J. Phys. Chem. C*, 117 (2013) 2709-2718.
- [45] Q. Jin, M. Fujishima, A. Iwaszuk, M. Nolan, H. Tada, Loading Effect in Copper(II) Oxide Cluster-Surface-Modified Titanium(IV) Oxide on Visible- and UV-Light Activities, *J. Phys. Chem. C*, 117 (2013) 23848-23857.
- [46] Q. Jin, M. Fujishima, M. Nolan, A. Iwaszuk, H. Tada, Photocatalytic activities of tin(IV) oxide surface-modified titanium(IV) dioxide show a strong sensitivity to the TiO₂ crystal form, *J. Phys. Chem. C*, 116 (2012) 12621-12626.
- [47] M. Nolan, First-Principles Prediction of New Photocatalyst Materials with Visible-Light Absorption and Improved Charge Separation: Surface Modification of Rutile TiO₂ with Nanoclusters of MgO and Ga₂O₃, *ACS Appl. Mater. Interfaces*, 4 (2012) 5863-5871.
- [48] A. Iwaszuk, M. Nolan, Reactivity of sub 1 nm supported clusters: (TiO₂)_n clusters supported on rutile TiO₂ (110), *Phys. Chem. Chem. Phys.*, 13 (2011) 4963-4973.
- [49] M. Nolan, Electronic coupling in iron oxide-modified TiO₂ leads to a reduced band gap and charge separation for visible light active photocatalysis, *Phys. Chem. Chem. Phys.*, 13 (2011) 18194-18199.
- [50] S. Rhatigan, M. Nolan, Impact of surface hydroxylation in MgO-/SnO-nanocluster modified TiO₂ anatase (101) composites on visible light absorption, charge separation and reducibility, *Chin. Chem. Lett.*, (2017) doi: 10.1016/j.cclet.2017.11.036

- [51] A. Lucid, A. Iwaszuk, M. Nolan, A first principles investigation of Bi₂O₃-modified TiO₂ for visible light Activated photocatalysis: The role of TiO₂ crystal form and the Bi³⁺ stereochemical lone pair, *Mater. Sci. Semicond. Process.*, 25 (2014) 59-67.
- [52] K.C. Schwartzberg, J.W.J. Hamilton, A.K. Lucid, E. Weitz, J. Notestein, M. Nolan, J.A. Byrne, K.A. Gray, Multifunctional photo/thermal catalysts for the reduction of carbon dioxide, *Catal. Today*, 280 (2017) 65-73.
- [53] U. Burghaus, Surface chemistry of CO₂ – Adsorption of carbon dioxide on clean surfaces at ultrahigh vacuum, *Prog. Surf. Sci.*, 89 (2014) 161-217.
- [54] S. Funk, T. Nurkic, B. Hokkanen, U. Burghaus, CO₂ adsorption on Cr(110) and Cr₂O₃(0001)/Cr(110), *Appl. Surf. Sci.*, 253 (2007) 7108-7114.
- [55] M.W. Abee, S.C. York, D.F. Cox, CO₂ Adsorption on α -Cr₂O₃ (1012) Surfaces, *J. Phys. Chem. B*, 105 (2001) 7755-7761.
- [56] O. Seiferth, K. Wolter, B. Dillmann, G. Klivenyi, H.J. Freund, D. Scarano, A. Zecchina, IR investigations of CO₂ adsorption on chromia surfaces: Cr₂O₃ (0001)/Cr(110) versus polycrystalline α -Cr₂O₃, *Surf. Sci.*, 421 (1999) 176-190.
- [57] H. Kuhlenbeck, C. Xu, B. Dillmann, M. Haßel, B. Adam, D. Ehrlich, S. Wohlrab, H.-J. Freund, U. A. Ditzinger, H. Neddermeyer, M. Neumann, M. Neuber., Adsorption and Reaction on Oxide Surfaces: CO and CO₂ on Cr₂O₃(111), *Berichte der Bunsengesellschaft für physikalische Chemie*, 96 (1992) 15-27.
- [58] M. Fronzi, M. Nolan, Surface Modification of Perfect and Hydroxylated TiO₂ Rutile (110) and Anatase (101) with Chromium Oxide Nanoclusters, *ACS Omega*, 2 (2017) 6795-6808.
- [59] G. Kresse, J. Hafner, *Ab initio* molecular dynamics for liquid metals, *Phys. Rev. B.*, 47 (1993) 558.
- [60] G. Kresse, J. Hafner, *Ab initio* molecular-dynamics simulation of the liquid-metal-amorphous-semiconductor transition in germanium, *Phys. Rev. B.*, 49 (1994) 14251-14269.
- [61] G. Kresse, J. Furthmüller, Efficiency of Ab-initio Total Energy Calculations for Metals and Semiconductors using a Plane-wave Basis Set, *Computational Materials Science*, 6 (1996) 15-50.
- [62] G. Kresse, J. Furthmüller, Efficient Iterative Schemes for Ab-initio Total-energy Calculations using a Plane-wave Basis Set, *Phys. Rev. B.*, 54 (1996) 11169.
- [63] G. Kresse, D. Joubert, From ultrasoft pseudopotentials to the projector augmented-wave method, *Phys. Rev. B.*, 59 (1999) 1758-1775.
- [64] P.E. Blöchl, Projector augmented-wave method, *Phys. Rev. B.*, 50 (1994) 17953-17979.
- [65] J.P. Perdew, J.A. Chevary, S.H. Vosko, K.A. Jackson, M.R. Pederson, D.J. Singh, C. Fiolhais, Atoms, molecules, solids, and surfaces: Applications of the generalized gradient approximation for exchange and correlation, *Phys. Rev. B.*, 46 (1992) 6671-6687.
- [66] S. Dudarev, G. Botton, S. Savrasov, C. Humphreys, A. Sutton, Electron-Energy-Loss Spectra and the Structural Stability of Nickel Oxide: An LSDA+U study, *Phys. Rev. B.*, 57 (1998) 1505.
- [67] J.J. Carey, M. Nolan, Enhancing the oxygen vacancy formation and migration in bulk chromium(III) oxide by alkali metal doping: a change from isotropic to anisotropic oxygen diffusion, *J. Mater. Chem. A*, 5, (2017) 15613 – 15630.
- [68] J.J. Carey, M. Legesse, M. Nolan, Low Valence Cation Doping of Bulk Cr₂O₃: Charge Compensation and Oxygen Vacancy Formation, *J. Phys. Chem. C*, 120 (2016) 19160-19174.
- [69] S. Posada-Pérez, F. Viñes, P.J. Ramirez, A.B. Vidal, J.A. Rodriguez, F. Illas, The bending machine: CO₂ activation and hydrogenation on δ -MoC(001) and β -Mo₂C(001) surfaces, *Phys. Chem. Chem. Phys.*, 16 (2014) 14912-14921.
- [70] NIST, NIST Standard Reference Database Number 69, NIST, 2017.